Regional Studies in Marine Science 78 (2024) 103770

Contents lists available at ScienceDirect

Regional Studies in Marine Science

journal homepage: www.elsevier.com/locate/rsma

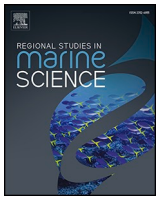

Massive mangrove dieback due to extreme weather impact - case of Maputo River Estuary, Mozambique

V.C. E. Machava-António [a,b,c,*], H. Mabilana [a], C. Macamo [a], A. Fernando [a], R. Santos [a,d], S. Bandeira [a], J. Paula [c]

[a] Department of Biological Sciences, Eduardo Mondlane University, P.O. Box 257, Maputo 1100, Mozambique
[b] United States Forest Service, International Programs, Maputo, Mozambique
[c] Mare – Marine and Environmental Research Centre, Faculty of Sciences, University of Lisbon, Campo Grande, Lisbon 1749-016, Portugal
[d] Centre of Marine Sciences of Algarve (CCMAR), University of Algarve, Gambelas Campus, Faro 8005-139, Portugal

ARTICLE INFO

Keywords:
Mangrove dieback
Ecosystem services
Change detection
Forest structure

ABSTRACT

This study documents one of the first massive mangrove dieback in Africa caused by hailstorm, occurring in Maputo Bay, Mozambique. Field observation and satellite imagery prompted this observation of extensive mangrove dieback out of Maputo River Estuary, a regionally significant large mangrove stand, the southernmost large mangrove area in the Western Indian Ocean.

This study aimed to determine the causes and extent of mangrove dieback in Maputo River Estuary that occurred in September 2019, identify, and quantify the mangrove loss, describe the structure of the mangrove forest, describe the soil composition in healthy and impacted areas. To address this Sentinel 2 imagery were assessed and calculated the Normalized Difference Vegetation Index (NDVI) to estimate the mangrove dieback area and cover change. This was supported by an extensive field survey, impacted and pristine or natural areas were assessed by sampling 233 plots of 10×10 m, established along transects separated by 50 m and set perpendicularly to the coastal line. Structural parameters assessed included species composition, height, diameter at the breast height (DBH), number of live and dead trees, density of stumps and seedling per species.

The mangrove cover reduced nearly half (48 %) of mangrove area in just a year, from 1377.4 Ha in 2019 to barely 716.2 Ha in 2020, representing a loss of 661.2 Ha, and 38.7 % of trees were completely dead. Five mangrove species were identified, *Avicenna marina* being largely dominant. The regeneration ratio was 142:10:1, way beyond the minimum ecological ratio of standard mangrove forest, 6:3:1. According to local communities and meteorological data, it seems plausible that this event was caused by a hailstorm.

These results contribute to understanding climate-related impacts on mangrove forests and its response which is crucial for adopting adequate management measures, recovery and climate change adaptation actions and monitoring of mangrove forests in Mozambique.

1. Introduction

The mangrove ecosystems are recognized among the most productive and biologically important ecosystems in the world as they provide valuable ecological, environmental, and economic benefits for the livelihoods of millions of people in coastal areas (Kathiresan and Bingham, 2001; FAO, 2007; Giri et al., 2011); Kauffman and Donato, 2012). Ecologically, mangroves support soil formation, photosynthesis, primary production, carbon storage, habitat provision for fishery nurseries, birds, and nutrients export (Cohen et al., 2013; UNEP, 2014). Mangroves also regulate ecological processes such as biological control, coastal protection, nutrient cycling, water quality regulation, erosion, wave attenuation, sediment accretion and maintenance of biodiversity (FAO, 2007; Cohen et al., 2013; UNEP, 2014).

Despite their recognized importance, mangrove forests are among the most threatened ecosystems worldwide because of natural and anthropogenic threats (Kuenzer et al., 2011; Taylor et al., 2003), with 35 % of the original global area being degraded or destroyed since 1980. Global rates of loss run between 1 % and 2 % per annum (Hagger et al., 2022; Duke et al., 2007; Valiela et al., 2001), and most recently the

* Corresponding author at: Department of Biological Sciences, Eduardo Mondlane University, P.O. Box 257, Maputo 1100, Mozambique.
E-mail address: vilma.machava@gmail.com (V.C.E. Machava-António).

https://doi.org/10.1016/j.rsma.2024.103770
Received 20 October 2023; Received in revised form 2 July 2024; Accepted 20 August 2024
Available online 22 August 2024

Global Mangrove Watch Version 3.0, estimated loss of 3.4 % of the global mangrove area between 1996 and 2020 (Bunting et al., 2022).

Climate change events are among the main reasons for natural mangrove loss in the last decades and are becoming more frequent in the 21st century, bringing significant impacts to coastal ecosystems (Kweku et al., 2018; Servino et al., 2018; Doney et al., 2012; (IPCC, 2001). Mangroves regularly experience multiple stressors that cause massive loss (Rossi et al., 2020), including changes in temperature, precipitation regimes and prolonged drought (Duke et al., 2017; Gilman et al., 2008; Asbridge et al., 2018; Servino et al., 2018) and are among the major climatic factors that may determine coastal wetland ecosystem extensions in the future (Gabler et al., 2017; Feher et al., 2017; Osland et al., 2017).

Mangrove's role in coastal protection has been emphasized in several studies in Mozambique, such as at the Save Delta, where they have protected the coastal village of Nova Mambone during Cyclone Eline (Macamo et al., 2016; Cabral et al., 2017). Modelling studies on mangroves vulnerability, focused on central Mozambique, were carried out (Charrua et al., 2020) as well as documentation of temporal changes of land use and cover due to Cyclone Idai (Bunting et al., 2023; Charrua et al., 2021).

Despite knowing the natural condition for mangrove colonization and development, it has been difficult to identify the causes of rapid, massive dieback of marshes and mangrove trees (Servino et al., 2018). These events have been associated with long-term stress on vegetation by sea level and drought (Asbridge et al., 2019; Servino et al., 2018; Levelock et al., 2017; Alongi, 2008), lunar cycles (Saintilan et al., 2022), associated with climate change effects (Lagomasino et al., 2021). Mangrove forests are resilient to multiple environmental changes and human impacts, but the capacity to detect and measure those impacts are still limited, with effects largely unstudied (Asbridge et al., 2019; Servino et al., 2018).

This study aims to determine the extension and causes of mangrove dieback in Maputo River Estuary and the impact of this loss on the ecosystem. To address this question, change detection was performed through spectral analysis of satellite images to (1) identify and quantify

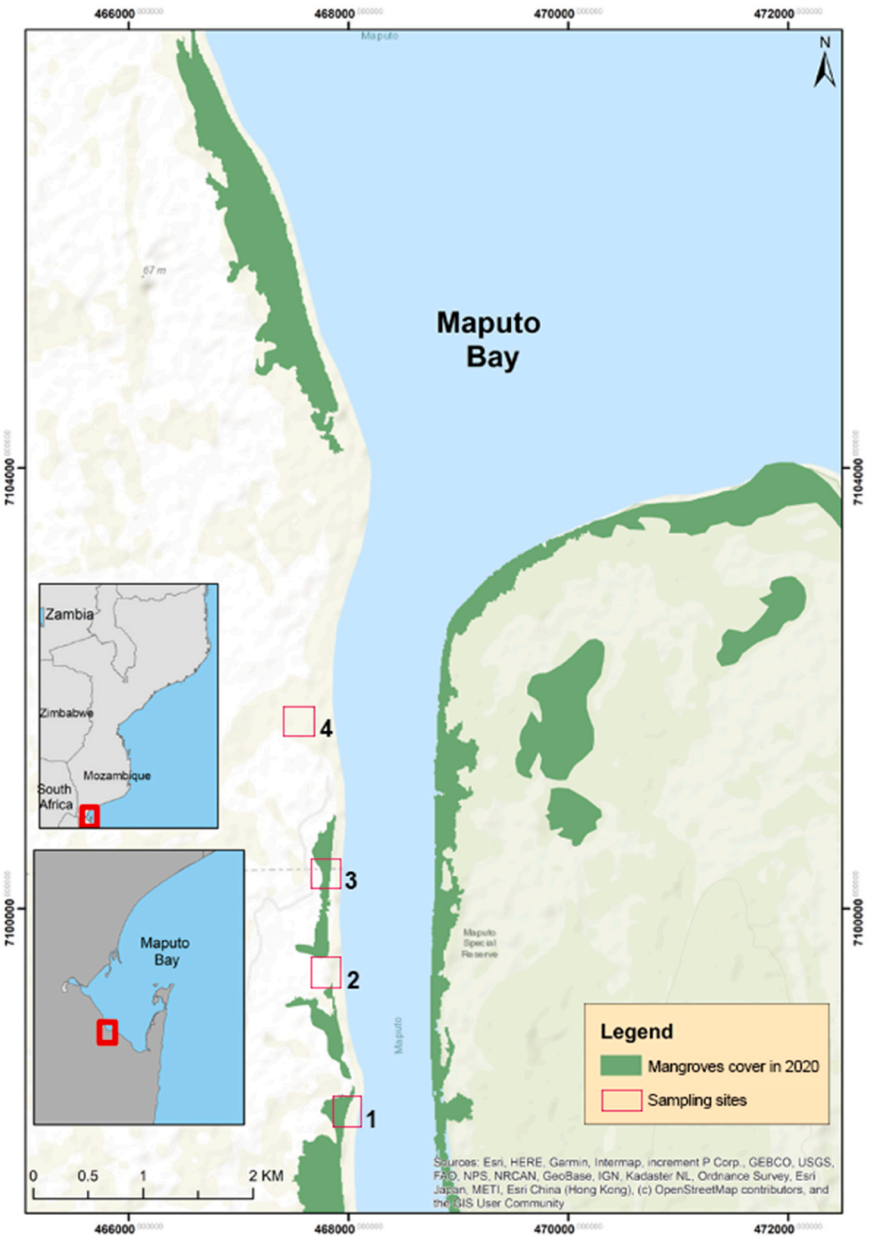

Fig. 1. Study area, Maputo River estuary.

the mangrove loss using a Normalized Difference Vegetation Index (NDVI, (Rouse et al., 1974; Pettorelli, 2013), (2) describe the structure of the mangrove forest in healthy and impacted areas, (3) describe the soil composition in healthy and impacted areas and (4) identify the causes of the mangrove dieback. This study addresses different commitments that Mozambique made, including the recommendations from the recently approved mangrove management strategy (Estratégia do Mangal, 2020–2024) and the millennium SDG 14 target. The results of this study will contribute to understanding the impact of climate change events, natural mangrove dieback and provide insights into adopting adequate mangrove recovery actions.

2. Materials and methods

2.1. Study area

The Maputo River estuary runs from south to northwards (see Fig. 1 below), and its lower basin is located in the coastal plains near the southern tip of Mozambique, in the south of Maputo Bay between 26º and 27ºS and 32º and 33ºE (MAE, 2005). The estuary opens to the southeast Maputo Bay area, one of the largest bays in eastern Africa with 1280 km^2, where mangroves occupy an area of 176 km^2 (Ferreira and Bandeira, 2014). Maputo Bay is an important fishing ground mainly because it has an extensive mangroves area and for being a shallow bay (with 10 m of depth on average) (Paula et al., 2014; Bosire et al., 2016).

The climate in the region is subtropical, with two seasons: a dry and cooler season from April to September and a wet and warm season from October to March. Maximum temperature in the wet season can reach 40 ºC, while in the dry season, it can go up to 28 ºC (Silva and Rafael, 2014). Precipitation varies between 34.7 – 211.9 mm in the wet season and 7.7 – 77.3 mm in the dry season (Fernando and Bandeira, 2009), with an annual average of approximately 884 mm (Dias et al., 2005). The humidity ranges from 50 % to 82 %, and salinity ranges from 30 – 39 with an annual average of 35 (Macamo et al., 2015).

2.2. Sampling methodology

2.2.1. Mangrove cover

Mangrove cover was assessed at a landscape scale through from Sentinel-2 imagery repository (Sentinel, 2014). Only the 10-meter resolution bands (band 2–4 and 8) were selected to the mapping exercise covering both visible (492.4 nm to 664.6 nm) and near infrared regions (832.8 nm) (Clevers and Gitelson, 2013; Sentinel, 2014; Pahlevan et al., 2017). Maximum likelihood Supervised classification algorithm was used to map mangrove cover before (June 2019) and after (June 2020) the mortality. Mangrove Class was extracted from both dates followed by a change detection analysis. The Normalized Difference Vegetation Index (NDVI: Rouse et al., 1974) that is the most utilized vegetation index (Pettorelli, 2013), was calculated using the formula:

$$NDVI = \frac{(NIR - Red)}{(NIR - Red)}$$

Where NIR is the near-infrared band and Red is the red band of spectral reflectance measurements.

Cloud-contaminated pixels can significantly decrease NDVI values (Holben, 1986), so images with cloud influence over the regions of interest were discarded. A field survey was conducted at impacted and natural Maputo River sites to validate the mangrove imagery data. The georeferenced survey sites were overlaid on the map, and then the field notes, photos and videos were compared with mapped damage level categories (Servino et al., 2018; Long et al., 2016). Information from the local communities regarding the mortality event was also taken to conduct the analysis.

2.2.2. Mangrove forest structure

Four sites were sampled along the Maputo River estuary, from the mouth (most impacted by the dieback) to the inner river. Plots were established and distributed in 50 m distant transects perpendicular to the coastal line in both impacted and non-impacted areas. Each plot had an area of 100 m^2 (10 m x 10 m), following standard field protocols (Macamo et al., 2018; Nicolau et al., 2017; Kauffman and Donato, 2012; Bandeira et al., 2009).

For each plot measurements included, the mangrove trees' height, species identity, diameter at the breast height (DBH), and the condition of each tree, defined in three categories: Intact trees = no sign of cutting, Partially Cut = less than 50 % of cut, Severally Cut = main stem cut or more than 50 % cut, and Stump = completely cut at the base, without healthy stems and/or branches (Kauffman and Donato, 2012; (Bandeira et al., 2009). The quality of the stem was also accessed, following the methodology used by Macamo et al. (2018), to determine the probability of being used or cut by local communities; Quality I - for trees with erect stems, there is a maximum probability of being used by local communities in their activities; Quality II - for trees with semi-erect stems, these would require some modification to be used; Quality III - for trees with very crooked stems, with no possibility of being used and also for dwarf trees whose stems are less than 1 m of height.

The number of live and dead trees and the height and density of stumps (Servino et al., 2018). Dead trees were defined by the absence of leaves, being classified into three classes: class 1= tree with small branches and twigs, class 2= absence of twigs or small branches and may have large branches, and class 3 = few or no branches, mostly stand stem or broken-topped (Kauffman and Donato, 2012).

Seedling species and number per quadrat were also registered and classified into 3 Regeneration Classes (RC) according to their height, RCI - seedlings less than 40 cm tall; RCII - with a height between 40 cm and 1.5 m; and RCIII - small plants with a height between 1.5 and 3 m (Bandeira et al., 2009; Kauffman and Donato, 2012; Macamo et al., 2018; Servino et al., 2018).

2.2.3. Sediment sampling and analysis

To compare sediment characteristics and evaluate possible impacts of mangrove dieback on the sediment Organic Matter (OM), two habitats (living and dead mangrove forest), each with two replicate sites were selected. Five samples were collected from each site, each consisting of a pool of 3 cores to reduce variability. Analyses were performed for two sediment layers (0–1 cm and 1–5 cm deep).

In the laboratory, the wet volume of each sediment sample was measured, and the dry weight density (g dw cm^{-3}) was determined by weighing the sample before and after being dried in an oven at 45ºC for 72 hours. Further sediment analyses were performed on subsamples from each replicate after homogenization (consisting of manually homogenizing in an agate mortar and then in a "Fritsh Planetary Ball" for 10 min).

For estimation of % Organic Matter (OM), approximately 5 g of each dry sample were placed in an aluminum container, and the container plus the subsample were weighted. The subsample and container were placed in the oven at 450°C for 4 hours.

OM was calculated as:

OM (%) = (dry weight – burnt weight)/ dry weight

2.3. Data treatment

Analysis of Variance was performed for (DBH (cm), height (m), and density (ind ha^{-1}), to compare stem quality, tree condition, and regeneration in living and dead mangrove areas. The Shapiro-Wilk normality test was used to evaluate data normality, and if significant, the nonparametric Kruskal–Wallis's test was used. The statistical analyses were performed using the software Stata Statistical Software, v10 and IBM SPSS Statistics, v25.0.

3. Results

3.1. Assessment of cause of mangrove dieback and change detection

During a preliminary visit to the field in November 2019 to the Maputo River area, a massive death in the mangrove area was observed, and the local communities and fishermen referred to a hailstorm event that occurred in September 2019, and according to the climate data from *Wordclim* (https://www.worldclim.org/data/monthlywth.html), this period had a minimum temperature of 15^0 C, maximum of 29^0 C, and 61 mm of precipitation, which is below the average temperature for the season of the year in this location. Local news also reported the occurrence of hailstorms on the same dates, although the National Meteorologic Institute don't have it recorded because it happened in a remote site without their coverage; and in the same year, a Category 4 storm, tropical Cyclone Idai, caused a massive mangrove dieback in central Mozambique.

The maps below show mangrove dynamics in the area between 2019, before mangrove dieback, and 2020, after the dieback (A and B, respectively). NDVI comparisons made for the sampling area, using data from 2019 and 2020, show a loss of 661.22 ha of forest area. In 2019, the mangrove extent in Maputo River was estimated at 1377.39 ha, while in 2020, the mangrove extent was estimated at 716.17 ha in the same area. In other words, in one year, the mangrove area in the Maputo River fell approximately 50 % (48.0 %) (Fig. 2).

Identifying and representing the areas where this 48.01 % loss of mangrove forest occurred was possible. Red lines show the area occupied by mangroves in 2019, and black lines indicate the area for 2020. The image shows that the area near the mouth was the most impacted by the loss, in the left and right margins of the estuary.

3.2. Mangrove forest structure

3.2.1. Structural parameters

Five species, including *Avicennia marina, Bruguiera gymnorhiza, Ceriops tagal, Rhizophora mucronata* and *Xylocarpus granatum* were recorded during the fieldwork. All five species were present only on site 4 (near the river mouth) and only four on the first three sites where *X. granatum* was not observed (Table 1). *Avicenna marina* was the dominant species in all four sites, with an Importance Value Index above 100, followed by *R. mucronata* on sites 1, 2 and 3, and *C. tagal* on site 4.

The forest has trees with an overall mean DBH of 16.6 ± 0.4 cm (mean ± SE) and a mean height of 2.32 ± 0.03 m. Structural parameters were not significantly different in all four sites, and the maximum DBH was found on site 2 (23.4 ±1.7 cm) compared to sites 1, 3 and 4 (Table 2). The forest has trees with heights varying from 2.0 m to 3.12 m. The maximum mean height was observed on site 3 (3.1 ±0.04 m), followed by sites 2, 1 and 4, with 3.0 ±0.1 m, 2.4 ±0.06 and 2.0 ±0.04, respectively (Table 2).

4. Stand density

The total mean stand density for the whole forest (sampled sites) was estimated at 1213.6 ±89.8 ind ha^{-1}. Site 1 had the highest mean, estimated at 1661.5 ±262.8 ind ha^{-1}, followed by sites 3 and 4 with 1356.7 ±217.55 ind ha^{-1} and 1204.6 ±126.6 ind ha^{-1}, respectively, and the minimum mean was found in site 2 with 659.3 ±100.5 ind ha^{-1} (Fig. 3). There are statistical differences when comparing the means for each site (Kruskal-Wallis H=14.096; gl=3, N=191, $p<0.05$).

Data from the density of the tree individuals by species have shown that, globally, *A. marina* had the highest density among sites 1, 2 and 4, and *R. mucronata* was the species with the highest density in site 3. The species with the second highest to the species with the minimum density are different depending on the sites.(Fig. 4)

Fig. 5 below shows the calculated mean density for all species found in Maputo River mangrove forest by sampling site. It is notable that in site 1, *A. marina* was the most abundant species (Fig. 6), with a mean density of 1348 ±271.5 ind ha^{-1} followed by *B. gymnorhiza* (840 ±132.7 ind ha^{-1}), *R. mucronata* (666.7 ±202.8) and *C. tagal* (325 ±143.6 ind ha^{-1}).

Despite having identified four species in Sites 2 and 3, only two species (*A. marina,* with 611.1 ±98.2 ind ha^{-1} and *B. gymnorhiza* with 300.0 ±100.0) had sufficient data for statistical analysis, and only three in Site 3, where the species with the highest density was *R. mucronata* (1922.2 ±456.1), followed by *A. marina* (810.7 ±107.6) and *B. gymnorhiza* (150.0 ±50.0). For site 4, *A. marina* (1157.94 ±127.8 ind ha^{-1}) had the highest density, followed by *R. mucronata* (616.67 ±271.31 ind ha^{-1}), *B. gymnorhiza* (420.0 ±226.7 ind ha^{-1}), and *C. tagal* (200.0 ±100.0 ind ha^{-1}) (*X. granatum* had insufficient data for statistical analysis). Shapiro-Wilk tests have shown normal distribution for all species densities ($p>0.05$). ANOVA comparison did not show any statistical difference between species densities in all four sampled sites.

5. DBH and height

The mangrove forest had 16.6 ±0.4 cm of DBH globally and 2.3 ±0.3 m height. Along the four sampled sites, trees' DBH varied between 15.3 ±0.5 cm in site 4, and 23.3 ±1.7 cm in site 2. Site 1 had a close DBH to Site 4 (Fig. 4), with 15.7 cm, while site 3 had 18.9 ±0.9 cm. Tree height varied between 2.0 ±0.0 m in site 4, and 3.1 ±0.1 m in site 3. In sites 1 and 2, trees' mean height was 2.4 ±0.1 m and 3±0.1 m, respectively (Fig. 6).

DBH and tree height data from this study did not show a normal distribution (Shapiro-Wilk (H=0.72; df=2081; $p<0.001$ and H=0.931; df=2081; $p<0.001$, respectively). Kruskal-Wallis for DBH did not find similarities between sites (Kruskal-Wallis' test: H (3, N=2320) = 95.02; $p<0.001$). However, pairwise comparisons found significant similarities when comparing sites 1 and 4, and sites 2 and 3 ($p>0.05$) (Table 3).

Comparisons for tree height also did not find similarities between sites (Kruskal-Wallis's test: H (3, N= 2081) =321.26; $p<0.001$). Pairwise Comparisons only found significant similarities when comparing site 2 and 3 ($p>0.05$) but did not find similarities comparing other sites ($p<0.05$) (Table 4).

The scatter plots show that trees are mostly young in all 4 sites sampled (Figs. 7 and 8). The highest density of trees in these locations is found in DBH classes ranging from 0 to 15 cm (Fig. 8). Statistical analysis also revealed that although there is a similar trend in the distribution of the diameter classes in the 4 sampled sites, there is a notable difference in the distribution and density of stumps (Fig. 8).

At sites 1, 2 and 3, most of the stumps sampled had diameters in the 0–15 cm range, while at site 4, the range with the highest stump density was 15–30 cm (Fig. 9: D).

5.1. Tree condition

It was found that 56.7 % of the trees sampled in Maputo River mangrove were dead trees (dieback), which was statistically significant (Kruskal-Wallis test: H (5, N= 4032) =147.52; p <0.001) when compared to other conditions, corresponding to 30.2 % Intact trees, 6 % Partially Cut (PC), 5.3 % Stump, 0.9 % Severally Cut (SC) and 0.9 %, Partially Dead trees (Fig. 9).

Out of the alive trees (intact), another characteristic visible in this forest was the presence of some intact and partially cut trees with a Dead Main Stem (DMS). The trees with DMS represented 0.80 % out of the 30.2 % intact trees in the forest, Partially Cut trees represented 6.0 %, and 0.1 % had a DMS.

In all sampled sites, the density of dead trees was high, with site 4 being the only one where the density of dead trees was higher than the density of living trees (Fig. 10) (intact, partially cut or severely cut), with an average of 278.7 ±38.8 tree ha^{-1} which corresponds to a ratio of 11:1 (Dieback: Living trees). Site 4 was located near Maputo River mouth, where the majority of the trees were dead or partially dead (20.2 ±5.3

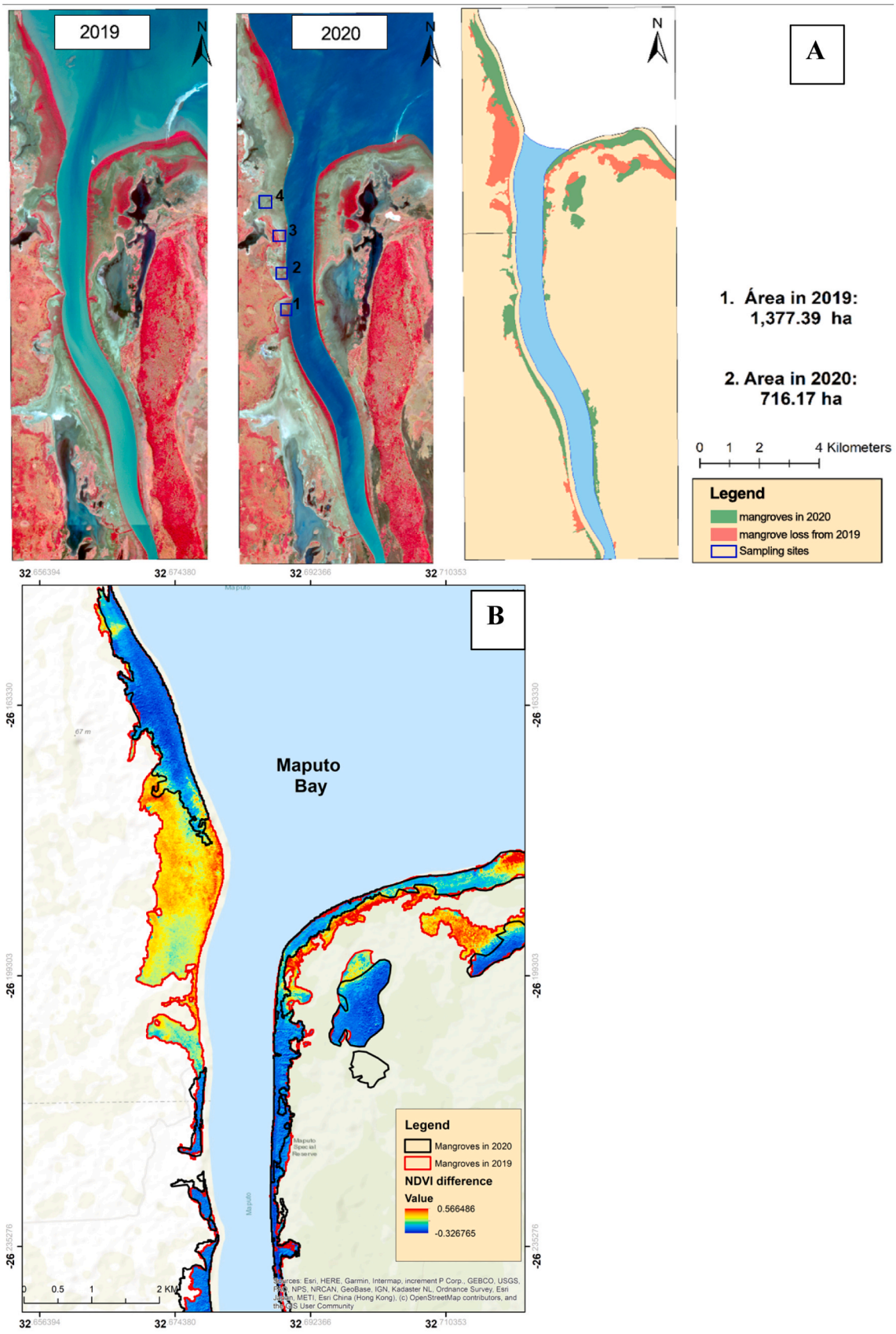

Fig. 2. Mangrove loss from 2019 to 2020. The first map (A) shows the mangrove area cover in 2019 and 2020, and the B the overlapping NDVI maps from 2019 and 2020.

Table 1
Importance Index Value for all mangrove species found in Maputo River.

Site	Species	Relative values			
		Density	Dominance	Frequency	IVI
Site 1	*Avicenna marina*	62.5	58.0	19.5	140.0
	Bruguiera gymnorhiza	12.5	8.4	2.4	23.4
	Ceriops tagal	10.0	16.3	0.8	27.6
	Rhizophora mucronata	15.0	17.3	2.3	34.6
Site 2	*Avicenna marina*	87.1	54.8	23.8	165.1
	Bruguiera gymnorhiza	6.5	9.6	0.8	16.9
	Ceriops tagal	3.2	4.7	0.3	8.2
	Rhizophora mucronata	3.2	30.9	0.7	34.8
Site 3	*Avicenna marina*	68.3	73.0	13.9	155.3
	Bruguiera gymnorhiza	4.9	3.8	0.2	8.8
	Ceriops tagal	4.9	8.9	0.3	14.0
	Rhizophora mucronata	22.0	14.3	10.6	46.9
Site 4	*Avicenna marina*	88.4	28.2	23.8	140.4
	Bruguiera gymnorhiza	4.1	6.5	0.4	11.0
	Ceriops tagal	1.7	34.5	0.2	36.3
	Rhizophora mucronata	5.0	3.0	0.7	8.7
	Xylocarpus granatum	0.8	27.9	0.0	28.7

tree ha^{-1}). Sites 1, 2 and 3 were the only sites with the highest density of intact trees (1334.6 ±36.5, 47.2 ±10.5 and 123.8 ±27.5 tree ha^{-1}), against dead trees (35.6 ±11.1, 14.8 ±6.0 and 38.3 ±8.9 tree ha^{-1}).

Sites 1 and 2 presented the same ratio for Dieback and living trees (1:6), the lowest ratio found in this forest, followed by the ratio found in site 3 (1:4). More than half of the dead trees were *A. marina*, corresponding to 53.4 % of the data, followed by *R. mucronata* (2.0 %), *B. gymnorhiza* and *C. tagal* with 0.8 % and 0.5 %. All partially dead trees found during sampling were *A. marina* (0.9 %). For intact trees, *A. marina* and *R. mucronata* were the most evident in the forest. These two species represented 19.4 % and 8.0 % of intact trees, respectively.

5.2. Tree quality

Observations in the field showed that most of the sampled trees had quality III stems, with the highest average found in site 1, 1311.5 ±238.7 tree ha^{-1}, followed by site 3, with 760 ±90 tree ha^{-1}, site 2 and site 1 with 504 ±85.14 tree ha^{-1} and 235.7 ±47.6 tree ha^{-1}, respectively.

A significant number of individuals corresponds to the quality I stems, with means ranging from 350.0 ±50.0 tree ha^{-1} and 671.4 ±202.0 tree ha^{-1} for sites 2 and 3, respectively, with the remaining individuals being those with quality II stems (211.1 ±42.3 tree ha^{-1} and 463.6 ±104.7 tree ha^{-1} for site 2 and 3, respectively). At sites 1 and 4, no individual with stem quality I was identified, but only individuals with quality II stems with an average of 133.3 ±33.3 tree ha^{-1} and 240.0 ±50.9 tree ha^{-1} for sites 4 and 1, respectively.

5.3. Regeneration

A total of 202 700 ind ha^{-1} of seedlings were identified, of which most individuals belonged to class I regeneration. Site 1 had the highest seedling density in class I with 4175.0 ±1720.8 ind ha^{-1}, followed by site 3, site 2 and site 4 (with means of 1 589.5 ±385.9 ind ha^{-1}; 1 428.6 ±311.3 and 1 154.6 ±196.7 ind ha^{-1}, respectively), at site 4 no seedlings in regeneration class III was identified (Fig. 11).

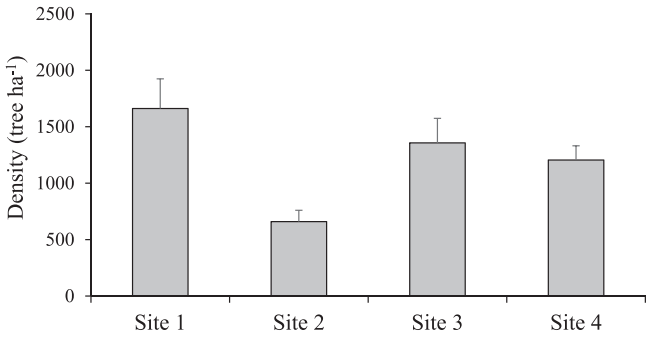

Fig. 3. Average density of trees in the three sampled sites.

Table 5 presents the percentage of seedlings in each different class per sampled site. Most of the seedlings fell into class I, most of which were planted by local communities after the dieback.

Shapiro-Wilk tests have shown that data are not normal for RCI ($p<0.05$) but are normal for the other regeneration classes ($p>0.05$). The comparative test Kruskal-Wallis (for RCI) and ANOVA (for RCII and RCIII) did not find any significant difference between groups ($p>0.05$). However, it was noticed that sites 1 and 2 were closer to the standard ratio compared to sites 3 and 4 (Table 6).

Local communities have been involved in restoration activities in the Maputo River area as illustrated in the Fig. 12 bellow. In the first picture, seedlings of *Ceriops tagal* and *Bruguiera gymnorhiza* planted have germinated and natural regeneration of other species such as *Avicennia marina* is also present. The second picture is of mangrove propagules planted in the severely impacted area where almost 100 % of those died and never germinated.

5.4. Organic matter assessment

In the dead mangrove, the percentage of Organic Matter (OM) in the 1st cm of sediment is lower than in the 1st cm of the live mangrove. This indicates that mangrove mortality resulted in a 30.0 % reduction in OM storage (8.4 % versus 11.9 %). Unlike the dead mangrove, in the live mangrove the percentage OM is higher on the surface. It is logical that the surface sediment has more OM than in-depth due to decomposition, that is, the OM of the oldest sediments was decomposed over a longer period (Fig. 13).

In the dead mangrove is different due to the recent reduction in OM sequestration caused by mangrove mortality. This observation supports the hypothesis that mangrove mortality reduced carbon sequestration and storage. The % OM of 1–5 cm is not significantly different between dead and live mangroves. This suggests that before mortality, the OM sequestration was similar in the two sites and consequently, the environmental conditions related to carbon sequestration were not different.

Table 2
Structural parameters.

	Site 1		Site 2		Site 3		Site 4	
	N=432	Q=40	N=178	Q=31	N=407	Q=41	N=1303	Q=121
Mean DBH (cm) ± SE	15.7	±0.9	23.4	±1.7	18.9	±0.9	15.3	±0.5
Mean Height (m) ± SE	2.4	±0.1	3.0	±0.1	3.1	±0.1	2.0	±0.04
Number of species	4		4		3		4	
Mean density (ind ha^{-1}) ± SE	1662	±262.8	659	±100.5	1357	±217.6	1205	±126.6
Basal Area (m^2 ha^{-1})	79.7		58.3		88.2		242.7	
Complexity Index	203.3		107.8		282.5		446.4	

Fig. 4. Aspect of dead mangrove forest in Maputo River (photos: Vilma Machava-António).

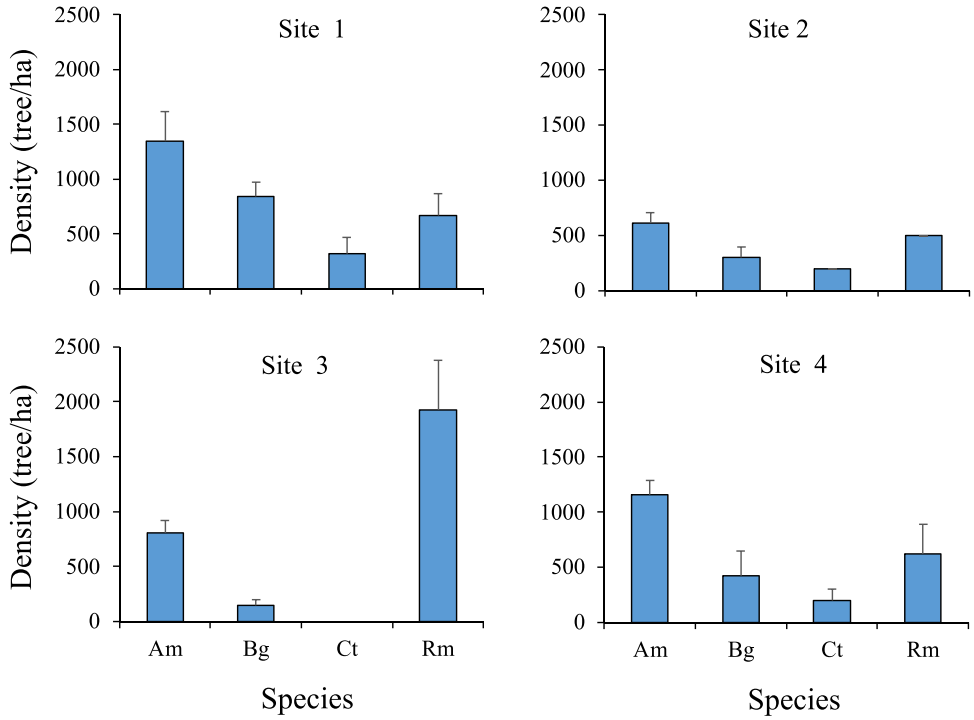

Fig. 5. Mean Density for all species sampled in all sampled sites. Am – Avicennia marina, Bg – Bruguiera gymnorhiza, Ct – Ceriops tagal, Rm – Rhizophora mucronata.

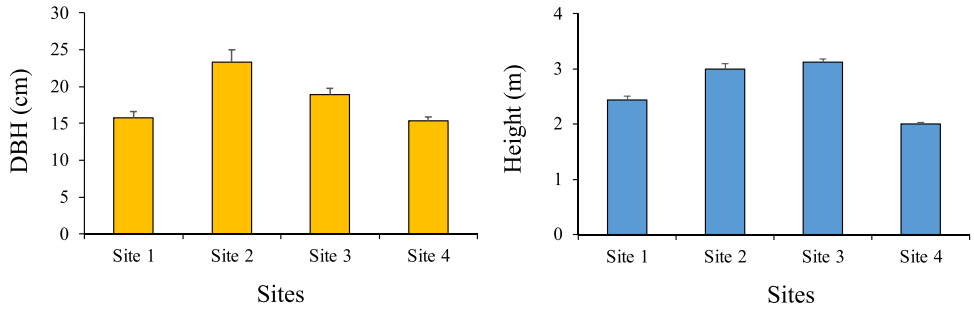

Fig. 6. Mean DBH (cm) and Height (m) for trees in all sampled sites.

Table 3
p-values from pairwise comparisons for DBH.

	Site 1	Site 2	Site 3
Site 2	<0.001		
Site 3	0.001	0.069	
Site 4	0.110	<0.001	<0.001

Table 4
Multiple comparison tests (P values) of the variable Height.

	Site 1	Site 2	Site 3
Site 2	<0.001		
Site 3	<0.001	1000	
Site 4	<0.001	<0.001	<0.001

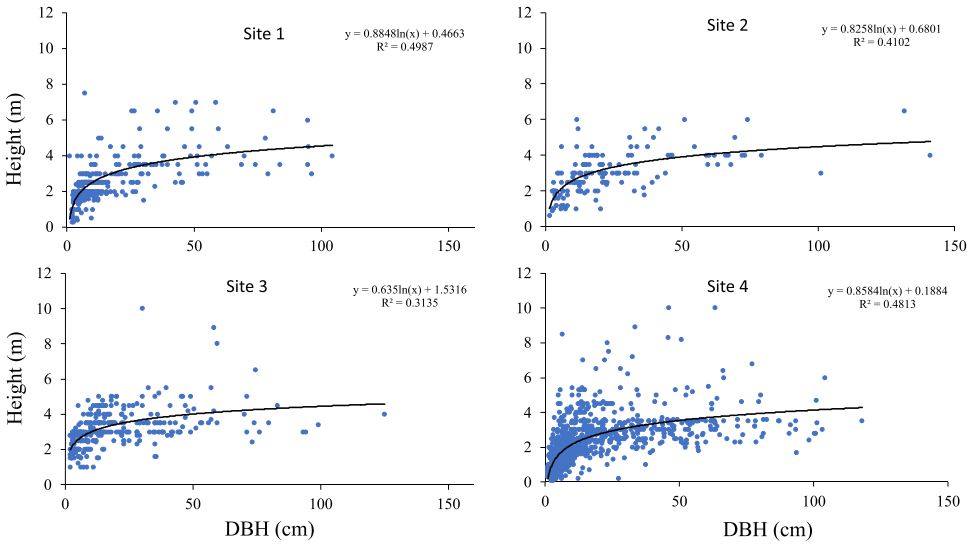

Fig. 7. Distribution of trees according to their Height and DBH.

6. Discussion

In 2019 the area of mangroves in the Maputo River estuary was estimated at 1 377.39 ha, and in 2020 the same area was estimated at 716.17 ha, meaning that in one year, the mangrove area in Maputo River estuary decreased by approximately 50 % (a loss of 661.22 ha) of the total area found in 2019. Approximately 70 % of published mangrove dieback events around the world are due to natural causes (Rossi et al., 2020) that occurred as a result of an extreme weather event (Duke et al., 2017; Asbridge et al., 2018; Servino et al., 2018), including the potential effects of climate change and increasing intensity of flood and drought events and frequency of storms (Macamo et al., 2016; Alongi, 2008; Gilman et al., 2008).

Using change detection tools, Sentinel 2 imagery and NDVI, this study documented for the first time a massive loss (nearly 50 %) of the mangrove area that has occurred in a short period of time (less than a year from 2019 to 2020). Elsewhere, with similar pattern of degradation and severity specially a dieback of around 50 % in short period of time caused by extreme weather impact was documented in Australia (Asbridge et al., 2018; Asbridge et al., 2019; Duke et al., 2017; Lovelock et al., 2017), in the USA (Florida) mangrove dieback due to the impact of Hurricane Irma (Lagomasino et al., 2021) and in Brazil caused by hailstorm impact (Servino et al., 2018). This study adds a new dimension in documenting mangrove loss due to climate-related events in Africa.

Climate change is likely to impact hailstorm frequency and size (Raupach et al., 2021) and such conditions may impact on canopy defoliation, bark damage and loss of floral buds and fruits (Houston, 1999; Clarke, 1992), a condition that might impact cause dieback.

Avicennia marina is dominant in southeast Africa, composing around 90 % of the trees (Macamo et al., 2015, Machava-António et al., 2022) and so does this study. *A. marina* was reported complete mortality due to climate change impact (Asbridge et al., 2019; Asbridge and Lucas, 2016).

The mangrove forest in Maputo Bay has been dominated by mostly young, short, and small trees with small DBH and low height. The average height of mangrove forests in early 2000 in Maputo Bay was 3.7 m, corresponding to the lowest average when compared to the provinces toward the north of Mozambique, more tropical which ranged between 4.0–15.9 m (Fernando and Bandeira, 2009; Fatoyinbo et al., 2008). Macamo et al. (Macamo et al., 2015) documented the mangrove forest in the Incomati Estuary (northern Maputo Bay) that had an average height of 2.6 m and an average DBH of 7.46 cm. And most recently, Machava-Antonio et al. (2022) who assessed mangrove forests in the entire bay, obtained the average height of the trees (1.74 ± 0.034 m) and the average DBH (6.89 ± 0.24 cm), suggesting that the forest structure parameters are decreasing in size. Globally mangrove fragmentation is commonly reported (Imbert, 2018), however antagonic data exists documenting both mangrove size decrease in this study and also increase in mangrove size.

The extension of the mangrove defoliation damage, the prospectus for recovery of the degraded mangrove and the rate of re-establishment thus seemingly depend on local environmental conditions (McCarthy et al., 2021; Radabaugh et al., 2020; Rivera-Monroy et al., 2019) and, especially the availability of seeds and seedlings (Kennedy et al., 2020); Alongi, 2009). This study documented the existence of many seedlings either from natural regeneration or active restoration conducted by communities (pers. Observation).

The study documented an abnormal ratio of 142:10:1, not approaching the standard minimum ecological ratio of 6:3:1 regeneration class. This ratio was also promoted by restoration which might not be efficient, as documented by other actors, where despite this initial recovery, there was mortality post-storm after some months (Fickert, 2020; Kennedy et al., 2020; Alongi, 2009), an indication that many seedlings never reach a size of a small plant (Macamo et al., 2018; Machava-António et al., 2022).

Mozambique's geographical location makes the coastal area vulnerable to extreme events of meteorological origin, such as droughts, floods, and tropical cyclones (FAO, 2007; MICOA, 2005). Several climate-related events affect different areas across the country (Charrua et al., 2020; Macamo et al., 2018), with highlight of the tropical Cyclone Idai that occurred in March 2019 in central Mozambique (Bunting et al., 2023; Charrua et al., 2021), but the evidence of hailstorm affecting mangrove areas is new or undocumented.

Local fishermen and community members, in the Maputo River estuary, reported that there was a hailstorm in the area in the month of September 2019, and after that the mangrove plants started dying massively and the dead condition continued for more than two years without signs of natural regeneration (Houston, 1999; Servino et al., 2018). The continued degradation after the hailstorm suggests that environmental stress persisted, as documented in studies about mangrove recovery after hailstorms and hurricanes that had a recovery period longer than one year (Roth, 1992; Houston, 1999; Long et al., 2016; Servino et al., 2018; Raupach et al., 2021).

The hailstorm damage to the Maputo River estuary impacted more than 50 % of the forest, and nothing similar has been documented in Southern Africa. Local communities conducted mangrove replantation.

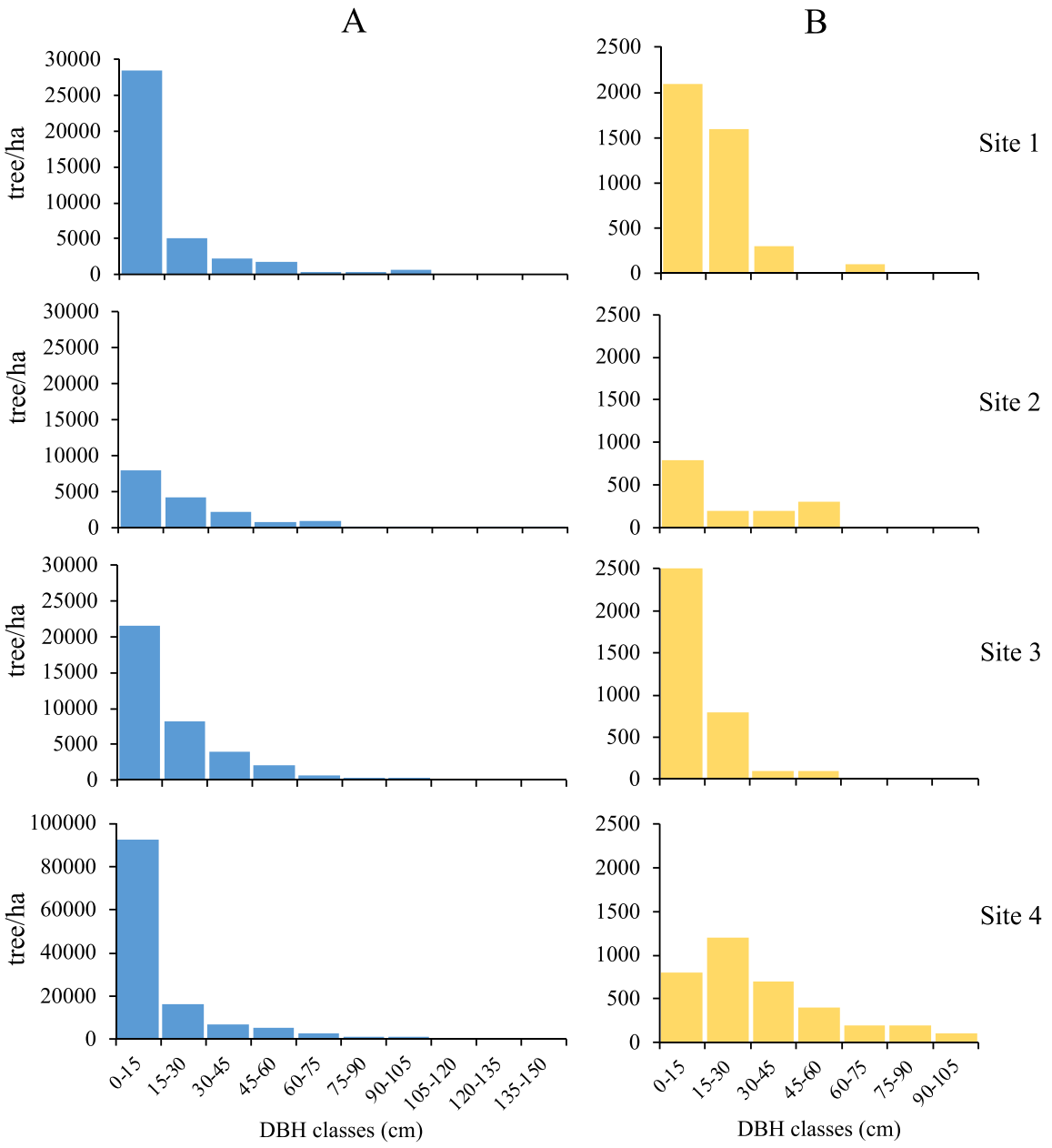

Fig. 8. Distribution of living trees in DBH classes. A, B, C and D, represent the distribution of stumps in DBH classes to the respective sites.

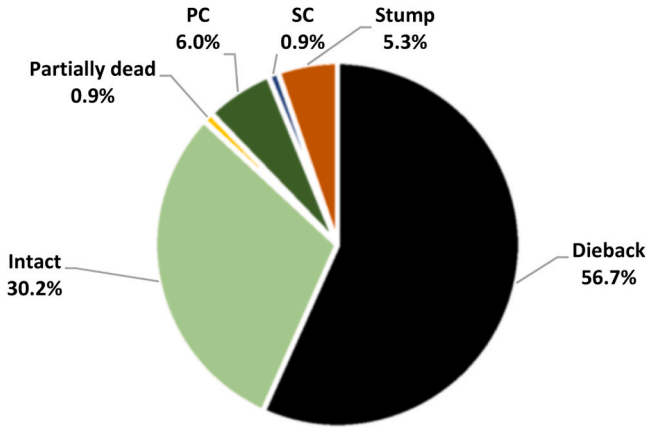

Fig. 9. Tree condition proportion in the sampled areas.

However, most of those die a few weeks after being planted, a scenario that can be caused by the soil condition that continues degrading even years after the dieback, with an absence of seedling growth and no regeneration of fresh leaves in the impacted sites (Servino et al., 2018), and these are among the major climatic factors that may determine coastal wetland ecosystem extensions in the future (Gabler et al., 2017; Feher et al., 2017; Osland et al., 2017).

In the Maputo River estuary, the soil composition was affected by the mangrove mortality, and the results of this study indicate that this mortality resulted in a 30.0 % reduction in OM storage. Furthermore, the surface sediment has more OM than in-depth due to decomposition, that is, the organic matter of the oldest sediments had more time to decompose, and the mangrove mortality reduced carbon sequestration. Before mortality, the OM sequestration was similar in the two sites and, consequently, the environmental conditions related to carbon sequestration were not different (Huston, 1999; Servino et al., 2018).

Survival and recovery of mangroves are influenced by soil salinization during drought events, where the reduction in freshwater input may

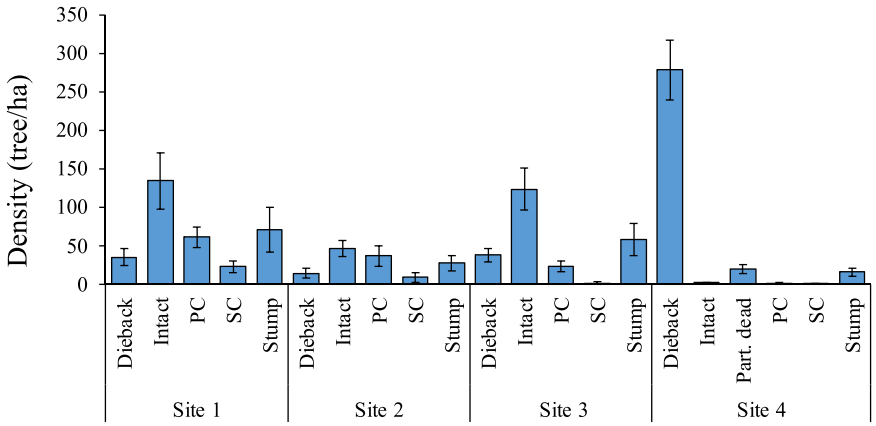

Fig. 10. Mean density for trees under different conditions found in all sites.

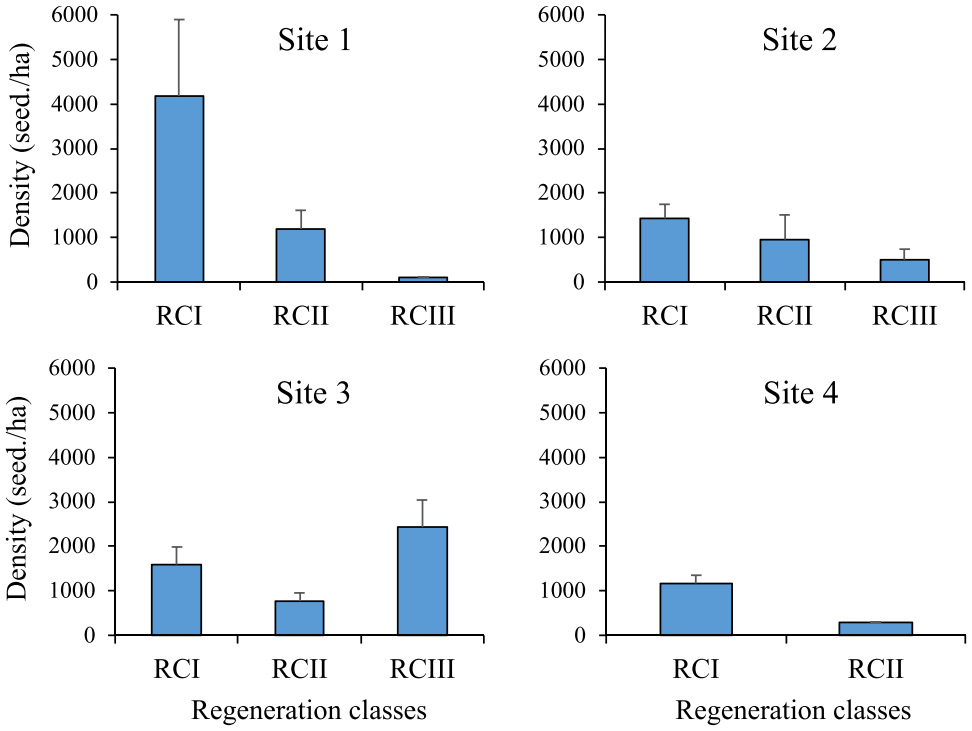

Fig. 11. Seedling densities within each regeneration class.

Table 5
Percentage of seedlings per regeneration class.

Percentage of seedlings per regeneration class			
	RCI	RCII	RCIII
Site 1	91.9 %	7.9 %	0.2 %
Site 2	76.5 %	19.6 %	3.8 %
Site 3	64.4 %	14.9 %	20.7 %
Site 4	98.8 %	1.2 %	

Table 6
Number of seedlings per regeneration class.

Seedlings per Regeneration class			
	RCI	RCII	RCIII
Site 1	418	36	1
Site 2	20	5	1
Site 3	3	1	1
Site 4	85	1	0

also impair mangrove health and recovery from water stress (Cintrón et al., 1978; Ball, 1988; Houston, 1999; MacKay et al., 2010).

The results of this study and the statement from the community indicate the need to assess the impact of this mangrove loss on the ecosystem services provided to the local community and the entire ecosystem, acquire techniques for appropriate restoration, assess the hydrology and engage communities in the restoration.

7. Conclusion

This study documents for the first time a massive mangrove dieback in Africa's sub-tropical context, contributing, therefore, to the wider understanding of this phenomenon. The assessment through local community members pointed to the September 2019 hailstorm as the cause of the mangrove's death. This extreme event might have started by damaging the mangrove trees' bark, concomitantly loss of floral buds

Fig. 12. Community restoration in a less impacted area (Site 1) and in the severely impacted area (Site 4).

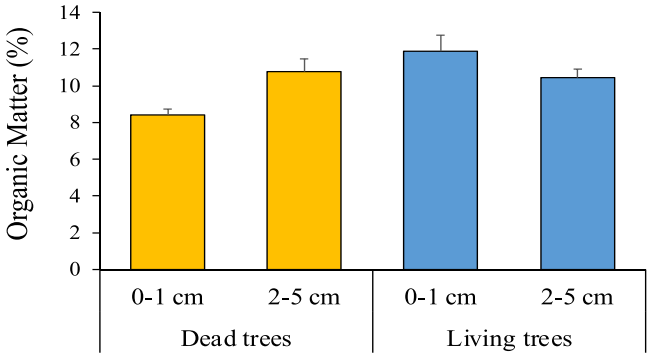

Fig. 13. Organic Matter in Dead vs Living mangrove trees.

and fruits and major canopy.

The mangrove cover was reduced by nearly half, from 1377.4 Ha in 2019 to barely 716.2 Ha in 2020, representing a loss of 661.2 Ha of mangrove area in just a year. In the sampled areas, 38.7 % of trees were completely dead. Five mangrove species were identified, *Avicenna marina* with the highest Importance Value Index, *B. gymnorhiza, C. tagal, R. mucronata* and *X. granatum*. The regeneration ratio was 142:10:1, way beyond the minimum ecological ratio of standard mangrove forest, 6:3:1. Mangrove dieback within Maputo Estuary triggered by hail in 2019 and has continued 2 years after having little or no sign of recovery.

Local communities conducted mangrove replantation in the impacted area, but most of the seedlings die before reaching 40 cm of height. These results contribute to understanding natural mangrove dieback, the adoption of adequate mangrove recovery actions, climate change adaptation actions and monitoring of mangrove forests in Mozambique.

CRediT authorship contribution statement

V.C. E. Machava-António: Writing – review & editing, Writing – original draft, Project administration, Methodology, Investigation, Funding acquisition, Conceptualization. **H. Mabilana:** Formal analysis. **C. Macamo:** Writing – review & editing, Methodology. **A. Fernando:** Formal analysis, Data curation. **R. Santos:** Methodology, Investigation. **S. Bandeira:** Writing – review & editing, Supervision. **J. Paula:** Writing – review & editing, Supervision.

Author statement

The authors declare that this manuscript is original, has not been published before and is not currently being considered for publication elsewhere.

Declaration of Competing Interest

The authors declare the following financial interests/personal relationships which may be considered as potential competing interests. Vilma Machava Antonio reports financial support was provided by Western Indian Ocean Marine Science Association. If there are other authors, they declare that they have no known competing financial interests or personal relationships that could have appeared to influence the work reported in this paper.

Data availability

Data will be made available on request.

Acknowledgements

Funding were provided by the Western Indian Ocean Marine Science Association (WIOMSA), under the MARG I grant number MARGI_2020_CO_42.

References

Alongi, D.M., 2008. Mangrove forests: resilience, protection from tsunamis, and responses to global climate change. Estuar. Coast. Shelf Sci. 76, 1–13. https://doi.org/10.1016/j.ecss.2007.08.024.

Asbridge, E.F., Bartolo, R., Finlayson, C.M., Lucas, R.M., Rogers, K., Woodroffe, C.D., 2019. 2019. Assessing the distribution and drivers of mangrove dieback in Kakadu National Park, northern Australia. Estuar., Coast. Shelf Sci. 228, 106353.

Asbridge, E., Lucas, R., Rogers, K., Accad, A., 2018. The extent of mangrove change and potential for recovery following severe Tropical Cyclone Yasi, Hinchinbrook Island, Queensland, Australia. Ecol. Evol. 8, 10416–10434.

Asbridge, E., Lucas, R.M., 2016. Mangrove response to environmental change in Kakadu national park. IEEE J. Sel. Top. Appl. Earth Obs. Remote Sens. 9, 5612–5620.

Ball, M., 1988. Ecophysiology of mangroves. Trees 2, 129–142 https://doi.org/10.1007/BF00196018.

Bandeira, S.O., Macamo, C.C.F., Kairo, J.G., Amade, F., Jiddawi, N., Paula, e J., 2009. Evaluation of mangrove structure and condition in two trans-boundary areas in the Western Indian Ocean. Aquat. Conserv. Mar. Freshw. Ecosyst. 19. S46–S55.

Bosire, J.O., Mangora M.M., Bandeira S., Rajkaran A., Ratsimbazafy R., Appadoo C., Kairo, J.G.. (eds.), 2016. Mangroves of the Western Indian Ocean: Status and Management. WIOMSA, Zanzibar Town, 161 pp.

Bunting, P., Hilarides, L., Rosenqvist, A., Lucas, R.M., Kuto, E., Gueye, Y., Ndiaye, L., 2023. Global mangrove watch: monthly alerts of mangrove loss for Africa. Remote Sens. 2023 15 (8), 2050. https://doi.org/10.3390/rs15082050.

Bunting, P., Rosenqvist, A., Hilarides, L., Lucas, R.M., Thomas, N., Tadono, T., Worthington, T.A., Spalding, M., Murray, N.J., Rebelo, L.-M., 2022. Global mangrove extent change 1996-2020: global mangrove watch version 3.0. Remote Sens. 2022 14 (15), 3657. https://doi.org/10.3390/rs14153657.

Cabral, P., Augusto, G., Akande, A., Costa, A., Amade, N., Niquisse, S., Atumane, A., Cuna, A., Kazemi, K., Mlucasse, R., Santha, R., 2017. Assessing Mozambique's exposure to coastal climate hazards and erosion. Int. J. Disaster Risk Reduct. 23, 45–52. https://doi.org/10.1016/j.ijdrr.2017.04.002.

Charrua, A.B., Bandeira, S.O., Catarino, S., Cabral, P., Romeiras, M.M., 2020. Assessment of the vulnerability of coastal mangrove ecosystems in Mozambique. Ocean Coast. Manag. 189, 105145 https://doi.org/10.1016/j.ocecoaman.2020.105145.

Charrua, A.B., Padmanaban, R., Cabral, P., Bandeira, S., Romeiras, M.M., 2021. Impacts of the tropical cyclone idai in mozambique: a multi-temporal landsat satellite imagery analysis. Remote Sens 13, 201 https://doi.org/10.3390/ rs13020201.

Cintrón, G., Lugo, A.E., Pool, D.J., Morris, G., 1978. Mangroves of arid environments in Puerto-Rico and adjacent islands. Biotropica 10 (2), 110–121. https://doi.org/10.2307/2388013.

Clarke, P.J., 1992. Predispersal mortality and fecundity in the grey mangrove (*Avicennia marina*) in south-eastern Australia. Aust. J. Ecol. 17, 161–168. https://doi.org/10.1111/j.1442-9993.1992.00794.

Clevers, J.G.P.W., Gitelson, A.A., 2013. Remote Estimation of Crop and Grass Chlorophyll and Nitrogen Content Using Red-edge Bands on Sentinel-2 and-3'. In: International Journal of Applied Earth Observation and Geoinformation, 23. Elsevier B.V, pp. 344–351. https://doi.org/10.1016/j.jag.2012.10.008.

Cohen, R., Kaino, J., Okello, J.A., Bosire, J.O., Kairo, J.G., Huxham, M., Mencuccini, M., 2013. Propagating uncertainty to estimates of above-ground biomass for Kenyan mangroves: a scaling procedure from tree to landscape level. For. Ecol. Manag. 310, 968–982.

Dias, J., e, Canhanga, S., 2005. Tidal characteristics of Maputo Bay, Mozambique. J. Mar. Syst. 58, 83–97.

Doney, S.C., Ruckelshaus, M., Duffy, J.E., Barry, J.P., Chan, F., Englidh, C.A., Galindo, H. M., Grebmeier, J.M., Hollowed, A.B., Knowlton, N., Polovina, J., Rabalais, N.N., Sydeman, W.J., Talley, L.D., 2012. Climate change impacts on marine ecosystems. Annu. Rev. Mar. Sci. 4, 11–37. https://doi.org/10.1146/annurev-marine-041911-111611.

Duke, N.C., Kovacs, J.M., Griffths, A.D., Preece, L., Hill, D.J.E., van Oosterzee, P., Mackenzie, J., Morning, H.S., Burrows, D., 2017. Large-scale dieback of mangroves in Australia's Gulf of Carpentaria: a severe ecosystem response, coincidental with an unusually extreme weather event. Mar. Freshw. Res. 68, 1816–1829. https://doi.org/10.1071/MF16322.

Duke, N.C., Meynecke, J.O., Dittmann, S., Ellison, A.M., Anger, K., Berger, U., Dahdouh-Guebas, F., 2007. A world without mangroves? Science 317 (5834), 41–42.

FAO., 2007. The world's mangroves 1980-2005. FAO forestry paper 153. Rome.

Ferreira, M., Bandeira, S., 2014. Maputo Bay's coastal habitats. In: Bandeira, S., Paula, J. (Eds.), The Maputo Bay Ecosystem. WIOMSA, Zanzibar Town, pp. 21–25.

Feher, L.C., Osland, M.J., Griffith, K.T., Grace, J.B., Howard, R.J., Stagg, C.L., Enwright, N.M., Krauss, K.W., Gabler, C.A., Day, R.H., Rogers, K., 2017. Linear and nonlinear effects of temperature and precipitation on ecosystem properties in tidal saline wetlands. Ecosphere 8, e01956. https://doi.org/10.1002/ecs2.1956.

Fickert, T., 2020. To plant or not to plant, that is the question: reforestation vs. natural regeneration of hurricane-disturbed mangrove forests in Guanaja (Honduras). Forests 11 (1068) (2020), 10.3390/f11101068.

Gabler, C.A., Osland, M.J., Grace, J.B., Stagg, C.L., Day, R.H., Hartley, S.B., Enwright, N. M., From, A.S., McCoy, M.L., McLeod, J.L., 2017. Macroclimatic change expected to transform coastal wetland ecosystems this century. Nat. Clim. Chang. 7, 142–147. https://doi.org/10.1038/NCLIMATE3203.

Gilman, E.L., Ellison, J., Duke, N.C., Field, C., 2008. Threats to mangroves from climate change and adaptation options: a review. Aquat. Bot. 89, 237–250.

Giri, C., Ochieng, E., Tieszen, L.L., Zhu, Z., Singh, A., Loveland, T., Masek, J., e, Duke, N., 2011. Status and distribution of mangrove forests of the world using earth observation satellite data. Glob. Ecol. Biogeogr. 20 (4), 154–159.

Hagger, V., Worthington, T.A., Lovelock, C.E., et al., 2022. Drivers of global mangrove loss and gain in social-ecological systems. Nat. Commun. 13, 6373. https://doi.org/10.1038/s41467-022-33962-x.

Holben, B.N., 1986. Characteristics of maximum-value composite images from temporal AVHRR data. Int. J. Remote Sens. 7, 1417–1434. https://doi.org/10.1080/01431168608948945.

Houston, W.A., 1999. Severe hail damage to mangroves at Port Curtis, Australia. Mangrove Salt Marshes 3, 29–40. https://doi.org/10.1023/A:1009946809787.

Imbert, D., 2018. Hurricane disturbance and forest dynamics in east Caribbean mangroves Ecosphere, 9 (7) (2018), p. e02231, 10.1002/ecs2.2231.

IPCC, 2001. In: Houghton, J.T., Ding, Y., Griggs, D.J., Noguer, M., van der Linden, P.J., Dai, X., Maskell, K., Johnson, C.A. (Eds.), Climate Change 2001: The Scientific Basis. Contribution of Working Group I to the Third Assessment Report of the Intergovernmental Panel on Climate Change.. Cambridge University Press, Cambridge, United Kingdom and New York, NY, USA, p. 881.

Kathiresan, K., Bingham, B.L., 2001. Biology of mangroves and mangrove ecosystems. Adv. Mar. Biol. 40, 81–251.

Kauffman, J.B., Donato, D.C., 2012. Protocols for the measurement, monitoring and reporting of structure, biomass, and carbon stocks in mangrove forests. In: Working Paper, 86. CIFOR, Bogor, Indonesia.

Kennedy, J.P., Dangremond, E.M., Hayes, M.A., Preziosi, R.F., Rowntree, J.K., Feller, I. C., 2020. 2020. Hurricanes overcome migration lag and shape intraspecific genetic variation beyond a poleward mangrove range limit. Mol. Ecol. 1–15. https://doi.org/10.1111/mec.15513.

Kuenzer, C., Bluemel, A., Gebhardt, S., Quoc, T.V., Dech, S., 2011. Remote sensing of mangrove ecosystems: a review. Remote Sens. (3), 878–928.

Kweku, Darkwah W., O. Bismark, A. Maxwell, K.A. Desmond, K.B. Danso, E.A. Oti-Mensah, A.T. Quachie and B.B. Adormaa. 2018. Greenhouse Effect: Greenhouse Gases and Their Impact on Global Warming. Journal of Scientific Research & Reports 17(6): 1-9, 2017; Article no. JSRR.39630 ISSN: 2320-0227. DOI: 10.9734/JSRR/2017/39630.

Lagomasino, D., Fatoyinbo, T., Castañeda-Moya, E., Cook, B.D., Montesano, P.M., Neigh, C.S.R., Corp, L.A., Ott, L.E., Chavez, S., Morton, D.C., 2021. Storm surge and ponding explain mangrove dieback in southwest Florida following Hurricane Irma. Nat. Commun. 12, 4003. https://doi.org/10.1038/s41467-021-24253-y.

Long, J., Giri, C., Primavera, J., Trivedi, M., 2016. Damage and recovery assessment of the Philippines' mangroves following Super Typhoon Haiyan. Mar. Pollut. Bull. 109, 734–743. https://doi.org/10.1016/j.marpolbul.2016.06.080.

Lovelock, C.E., Feller, I.C., Reef, R., Hickey, S., Ball, M.C., 2017. Mangrove dieback during fluctuating sea levels. - PubMed - NCBI. Sci. Rep. -uk 7, 129. https://doi.org/10.1038/s41598-017-01927-6.

Macamo, C., Adams, J., Mabilana, H., Bandeira, S., Machava Antonio, V., 2018. Spatial dynamics and structure of human disturbed mangrove forests in contrasting coastal communities in eastern Africa. Wetlands. https://doi.org/10.1007/s13157-018-0996-7.

Macamo, C., Balidy, H., Mandeira, S., Kairo, e J., 2015. Mangrove Transformation in the Incomati Estuary, Maputo Bay, Mozambique. In: WIO Journal of Marine Science, Vol. 14, pp. 11–22.

Macamo, C., Bandeira, S., Muando, S., de Abreu, D., and Mabilana, H.. 2016. Mangroves of Mozambique. In: Bosire J. O., Mangora M. M., Bandeira S., Rajkaran A., Ratsimbazafy R., Appadoo C., and Kairo J. G. 2016. Mangroves of the Western Indian Ocean: Status and Management. WIOMSA, Zanzibar Town, pp. 51-73.

MacKay, F., Cyrus, D., Russell, K.L., 2010. Macrobenthic invertebrate responses to prolonged drought in South Africa's largest estuarine lake complex. Estuar. Coast. Shelf Sci. 86, 553–567. https://doi.org/10.1016/j.ecss.2009.11.011.

MAE, 2005. (Ministério da Administração Estatal). Perfil do Distrito de Matutuine, Província de Maputo. República de Moçambique.

McCarthy, M.J., Jessen, B., Barry, M.J., Figueroa, M., McIntosh, J., Murray, T., Schmid, J., Muller-Karger, F.E., 2021. Automated high-resolution time series mapping of mangrove forests damaged by hurricane Irma in southwest Florida Rem. Sens 12 (1740). https://doi.org/10.3390/rs12111740.

MICOA. Avaliação da Vulnerabilidade as Mudanças Climáticas e Estratégias de Adaptação; Ministry of Environment, Government of Mozambique: Maputo, Mozambique, 2005.

Nicolau, D.K., Macamo, C.C., Bandeira, S.O., Tajú, A., Mabilana, H., 2017. Mangrove change detection, structure, and condition in a protected area of eastern Africa: the case of Quirimbas National Park, Mozambique. WIO J. Mar. Sci. 16 (1), 47–60.

Osland, M.J., Feher, L.C., Griffith, K.T., Cavanaugh, K.C., Enwright, N.M., Day, R.H., Stagg, C.L., Krauss, K.W., Howard, R.J., Grace, J.B., Rogers, K., 2017. Climatic controls on the global distribution, abundance, and species richness of mangrove forests. Ecol. Monogr. 87, 341–359. https://doi.org/10.1002/ecm.1248.

Pahlevan, N., S. Sarkar, B.A. Franz, S.V. Balasubramanian, and J. He., 2017. Sentinel-2 MultiSpectral Instrument (MSI) data processing for aquatic science applications: Demonstrations and validations, Remote Sensing of Environment, Volume 201, 2017, Pages 47-56, ISSN 0034-4257, https://doi.org/10.1016/j.rse.2017.08.033.

Paula, J., Macamo, C., Bandeira, S., 2014. Mangroves of Maputo Bay. In: Bandeira, S., Paula, J. (Eds.), In: The Maputo Bay Ecosystem. WIOMSA, Zanzibar Town, pp. 109–146.

Pettorelli, N., 2013. The Normalized Difference Vegetation Index. OUP, Oxford (224 pp.). PMA (Prefeitura Municipal de Aracruz), 2013. Lei n° 3.739 – Altera a categoria da Unidade de Conservação Reserva Ecológica dos Manguezais Piraquê-Açú e Piraquê-Mirím para Reserva de Desenvolvimento Sustentável Municipal Piraquê-Açú e Piraquê-Mirím no município de Aracruz, Estado do Espírito Santo, e das outras providências (5 pp.).

Radabaugh, K.R., Moyer, R.P., Chappel, A.R., Dontis, E.E., Russo, C.E., Joyse, K.M., Bownik, M.W., Goeckner, A.H., Khan, N.S., 2020. Mangrove damage, delayed mortality, and early recovery following hurricane Irma at two landfall sites in Southwest Florida. USA Estuar. Coast 43, 1104–1118. https://doi.org/10.1007/s12237-019-00564-8.

Raupach, T.H., Martius, O., Allen, J.T., Kunz, M., Lasher-Trapp, S., Mohr, S., Rasmussen, K.L., Trapp, R.J., Zhang, Q., 2021. The effects of climate change on hailstorms. Nat. Rev. Earth Environ. 2 (3), 213–226. https://doi.org/10.1038/s43017-020-00133-9.

Rivera-Monroy, V.H., Danielson, T.M., Moya, E.C., Marx, B.D., Travieso, R., Zhao, X., Gaiser, E.E., Farfan, L.M., 2019. Long-term demography and stem productivity of Everglades mangrove forests (Florida, USA): resistance to hurricane disturbance. For. Ecol. Manag. 440, 79–91. https://doi.org/10.1016/j.foreco.2019.02.036.

Rossi, R.E., Archer, S.K., Giri, C., Layman, C.A., 2020. The role of multiple stressors in a dwarf red mangrove (Rhizophora mangle) dieback. Estuar., Coast. Shelf Sci. 237 (2020), 106660 https://doi.org/10.1016/j.ecss.2020.106660.

Roth, L.C., 1992. Hurricanes and mangrove regeneration: effects of hurricane Joan, October 1988, on the vegetation of Isla del Venado, Bluefields, Nicaragua. Biotropica 24, 375–384.

Rouse, J.W., Haas, R.H., Schell, J.A., e, Deering, D.W., 1974. Monitoring Vegetation systems in the Great Plains with ERTS. Third Earth Resour. Technol. Satell. (ERTS) Symp. 1, 48–62.

Saintilan, N., Lymburner, L., Wen, L., Haigh, I.D., Ai, E., Kelleway, J.J., Rogers, K., Pham, T.D., Lucas, R., 2022. The lunar nodal cycle controls mangrove canopy cover on the Australian continent. Sci. Adv. 8, eabo6602. https://doi.org/10.1126/sciadv.abo6602.

Sentinel, E.S.A. (2014) 'Missions-Sentinel Online', ESA: Paris, France.

Servino, R.N., de Oliveira Gomes, L.E., Bernardino, A.F., 2018. Extreme weather impacts on tropical mangrove forests in the Eastern Brazil Marine Ecoregion. Sci. Total Environ. (2018), 233–240, 628–629.

Silva, A., and J. Rafael. Geographical and Socio-Economic Setting of Maputo Bay. In: Bandeira, S. and Paula, J. 2014. The Maputo Bay Ecosystem. WIOMSA, Zanzibar Town, pp 11 – 19.

Taylor, M., Ravilious C. and Green, E.P. 2003. Mangroves of East Africa, UNEP, World Conservation Monitoring Centre, 26pp.

UNEP. 2014. The Importance of Mangroves to People: A Call to Action. van Bochove, J., Sullivan, E., Nakamura, T. (Eds). United Nations Environment Programme World Conservation Monitoring Centre, Cambridge. 128 pp.

Valiela, I., Bowen, J., York, J., 2001. Mangrove forests: one of the world's threatened major tropical environments. BioScience 51, 807–815.